Applied Physics A (2023) 129:327
https://doi.org/10.1007/s00339-023-06608-y

Applied Physics A
Materials Science & Processing

S.I. : 50TH ANNIVERSARY OF APPLIED PHYSICS

Laser engineered polymer thin films as drug delivery systems

A. Bonciu[1] · L. Cremer[2] · A. Calugaru[2] · E. Vlase[2] · C. Coman[2] · Alexandra Palla-Papavlu[1] · Dan Alin Cristian[3,4] · F. Grama[3,4]

Received: 4 January 2023 / Accepted: 24 March 2023 / Published online: 7 April 2023

Abstract
This study is focused on the fabrication of thin films of hydroxypropyl methylcellulose (HPMC) and ethyl cellulose (EC) polymer blends impregnated with captopril via matrix assisted pulsed laser evaporation (MAPLE) for the design of transdermal patches. The laser engineered polymer blend: captopril films are evaluated for physicochemical characteristics such as film morphology, chemistry of the films surface, drug content, and in vivo animal irritancy and skin sensitivity studies. The morphological investigation of the MAPLE fabricated coatings, i.e., by atomic force microscopy reveals that the morphology and topography of the polymer: drug films may be tuned by adjusting the HPMC: EC ratio in the MAPLE target. In addition, by tuning the HPMC: EC ratio in the as-deposited MAPLE films, it is possible to adjust the drug release profile. The Fourier-transform infrared spectroscopy investigation showed no interaction between captopril and the polymers (HPMC: EC) used. The skin irritation studies carried out on rabbits, showed no noticeable skin reactions, thus pointing out the compatibility of captopril with both the polymer blend and with the skin. In addition, no skin sensitization was noted among the guinea pigs that were challenged with the MAPLE fabricated transdermal patches. To sum up, the application of matrix-assisted pulsed laser evaporation for the fabrication of hydrophilic: hydrophobic polymer blends shows that there is great potential for the development of transdermal drug delivery system of captopril.

Keywords Captopril · Transdermal patches · Matrix-assisted pulsed laser evaporation · Laser · MAPLE · Hydroxypropyl methylcellulose · HPMC · Ethyl cellulose · EC · Drug delivery · Blends

1 Introduction

Drug delivery to patients for the treatment of acute or chronic diseases has been mostly accomplished using drug carriers like injectables, capsules, or tablets. Transdermal patches are alternative drug delivery systems, which are applied on the skin and are able to provide the controlled release of a drug, for the systemic treatment of the disease [1, 2]. They are designed to support the passage of drug substances from the surface of the skin, through its various layers and into the systemic circulation [3]. The advantages of the transdermal patches over its oral counterpart arise from the fact that they can offer a controlled release of the drug to the patient, enable a steady blood level profile, and a better patience compliance by avoiding hepatic first pass metabolism and effectiveness [4, 5]. Furthermore, the dosage form of transdermal patch is user friendly, convenient and offers multi-day dosing [6].

Transdermal patches are available on the pharmaceutics market since the 1980s, and are particularly important for the treatment of chronic diseases such as hypertension [7]. Hypertension is one of the most spread heart conditions, most commonly treated by oral medications, i.e., captopril (Catapres-TTS® (ALZA Corporation, Vacaville, CA, USA) [8]. Captopril is used in chronical treatment of hypertension and congestive heart failure as first agent, because of the absence of side effects in the majority of patients. The

✉ Alexandra Palla-Papavlu
alexandra.papavlu@inflpr.ro

✉ Dan Alin Cristian
dancristi@gmail.com; Daniel.cristian@umf.ro

[1] National Institute for Lasers, Plasma, and Radiation Physics, Atomistilor 409, 077125 Magurele, Romania

[2] "Cantacuzino" National Medico-Military Institute for Research and Development, Bucharest, Romania

[3] "Carol Davila" University of Medicine and Pharmacy, Bucharest, Romania

[4] General Surgery Department, Colțea Hospital, Bucharest, Romania

drug is an orally effective angiotensin I converting enzyme inhibitor [9]. However, long term therapy of hypertension by captopril on oral administration generally results in poor patient compliance due to the low bioavailability and short plasma half-life requiring increased frequency of drug administration [10].

The various properties of captopril are very suitable for a transdermal therapeutic system i.e., comparatively short elimination half-life and its oxidation rate in dermal homogenate is significantly lower than that in intestinal homogenate, low molecular weight (217.29 Da), low melting point (105–108 °C) and low daily therapeutic dose (50–75 mg) [9]. Captopril has a relatively short elimination half-life in plasma (1–3 h) and low oral bioavailability (60–75%). For these reasons, by applying this drug as a transdermal therapeutic system, dosing time intervals will be expanded [11]. However, to design efficient and cost-effective transdermal patches, all these possible benefits must be weighed against potential disadvantages. For example, there are some critical considerations to be taken into account for the optimization of a transdermal patch, such as its compatibility with the skin, and physical or chemical stability of the formulation and its components [12, 13]. Thus, material selection and fabrication techniques are crucial for the design of an efficient controlled drug release system based on transdermal patches.

The combination of hydrophilic:hydrophobic polymers are gaining increasing attention for their usage in controlled drug release systems. This is due to the possibility to tailor the drug release by changing the viscosity, substitution type and concentration of the hydrophilic polymer [14, 15].

Hydroxypropyl methylcellulose (HPMC): ethylcellulose (EC) blend was chosen for our approach, because it accrues both advantages of HPMC and EC. HPMC is frequently used due to the fact that is responsible for the formation, by hydration, of a diffusion and erosion-resistant gel layer which is able to control drug release [16]. EC is a non-toxic, stable, compressible, inert, hydrophobic polymer used for the fabrication of different drug release systems including tablets [17] or microcapsules [18]. Although there are numerous studies available on the realization of transdermal patches, there are still various questions to be answered and many parameters to be optimized. For example, rashes, local irritation or erythema could appear as a result of the drug, the adhesive, or excipients in the patch formulation. Moreover, the physicochemical properties of the drugs to be delivered are very important as only drugs with a lipophilic character can cross the stratum corneum, and ionic drugs cannot be delivered using transdermal route. In addition, transdermal drug delivery system cannot achieve high drug levels in blood/plasma [19, 20].

Thus, the aim of this study is focused on the realization of new proof-of-concept transdermal patches by using an alternative fabrication technology based on lasers, i.e., matrix assisted pulsed laser evaporation (MAPLE) [21–25]. Briefly, MAPLE is a thin film deposition technique similar to the pulsed laser deposition [26], with a different procedure for target fabrication. In PLD, the laser beam interacts with a target material, resulting in the formation of a plasma plume that is transporting the ablated species to a substrate placed parallel to the target. In MAPLE, the target consists in suspending the guest material in a solvent which is named matrix, and flash-freezing in liquid nitrogen the mixture resulting in a solid target. MAPLE has some advantages over the classical PLD, which arise mainly from the fact that in MAPLE, the matrix absorbs the laser radiation, there are no photochemical interactions between the matrix and the guest material, and ultimately, the guest material is collected, as a thin film onto the substrate. MAPLE has been already demonstrated for the successful deposition of polymer coatings [27, 28], polymer blends [29, 30], nanoparticles [31], and even polymer: carbon nanotube films [32].

The objective of the present work is to formulate matrix transdermal patches of captopril, to evaluate and establish their physico-chemical characteristics as well as their drug release profile, together with the skin irritancy and sensitization potential. With this research study we aim at advancing the optimization of transdermal therapeutic systems via novel laser-based approaches. In addition, this study could contribute to the understanding of laser-polymer-drug interactions and open new avenues for biomaterial development.

2 Materials and methods

2.1 Materials

Ethylcellulose (EC), i.e., the most insoluble cellulose derivative, and hydroxypropyl methylcellulose (HPMC) (hydrophilic polymer) are chosen as materials for the fabrication of thin films via matrix-assisted pulsed laser deposition (MAPLE). Captopril (Cp) is a well-established antihypertensive drug that is available in oral dosage form and could benefit from transdermal drug delivery. All materials are obtained from Sigma-Aldrich and used without further purification. The chemical formulas of ethylcellulose, hydroxypropyl methylcellulose, and captopril are shown in Fig. 1.

Double distilled water, toluene, and ethanol are also obtained from Sigma-Aldrich and used as matrices without further purification. The polymers are suspended in the compatible solvents (EC in toluene: ethanol 80:20 wt%, HPMC in distilled water, two different experiments) to 1 and 2 wt% solutions and then flash frozen in liquid nitrogen resulting in solid targets which are used in the MAPLE experiments.

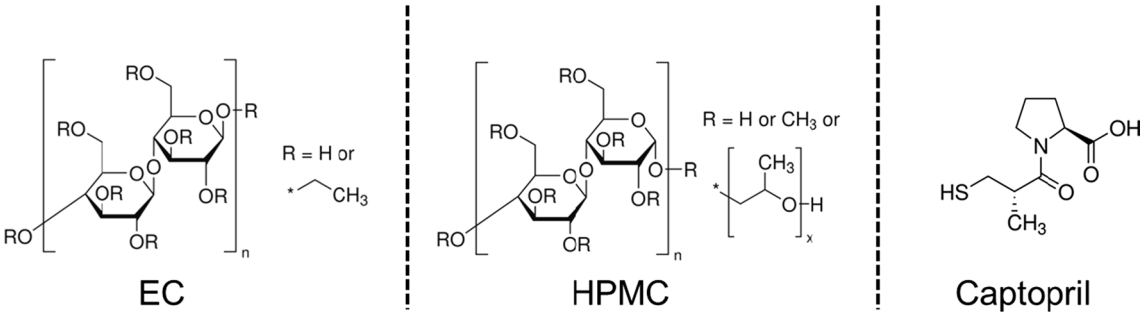

Fig. 1 Chemical structure of the materials used for laser processing

2.2 Preparation of patches via matrix assisted pulsed laser evaporation (MAPLE)

In this work, we aim at the fabrication of a proof-of-concept transdermal therapeutic system via matrix assisted pulsed laser evaporation. Here, the forth harmonic (266 nm laser wavelength) of a "Surelite II" pulsed Nd:YAG laser system (Continuum Company) is used to irradiate the frozen (polymer blend: drug): solvent target. The target is rotated with a motion feedthrough driven by a motor resulting in the laser beam describing a circle onto the sample to achieve uniform evaporation. The laser fluence is set at 500 mJ/cm^2. The polymer blend: drug thin film depositions are carried out in vacuum, at a background pressure ranging from 7×10^{-5} to 2×10^{-4} mbar, obtained with a Pfeiffer-Balzers TPU 170 turbomolecular pump (170 Ls^{-1}). During some depositions the pressure varied probably due to outgassing of the targets under vacuum. A scheme of the experimental setup is shown in Fig. 2 [32]. The number of pulses is varied between 96,000 and 100,000, resulting in polymer blend: drug films with thickness of around 500 nm thick. The substrates are kept at ambient temperature during the depositions and are placed at a distance of 4 cm from the frozen target. For the MAPLE experiments, two types of substrates are used: (1) double polished silicon substrates Si(100) cut into 1 cm^2 samples, which are transparent in the IR further and which are used for post-characterization; (2) flexible polyimide substrates which are further used for the in vivo tests.

All substrates used in both types of experiments are cleaned prior to any deposition. The substrates are ultrasonicated in successive baths of acetone and ethanol, followed by rinsing them several times in the ultrasonic bath with ultrapure water (0.2 µm filtered). They are finally dried in a nitrogen flow.

2.3 Animals

2.3.1 Ethics statement

This study on animals is carried out in compliance with the principles of ethics and in accordance with the provisions of EU Directive 63/2010 on compliance with the rules for the care, use, and protection of animals used for scientific purposes.

The study has been favorably evaluated by the Ethics Committee of the "Cantacuzino" National Medical-Military

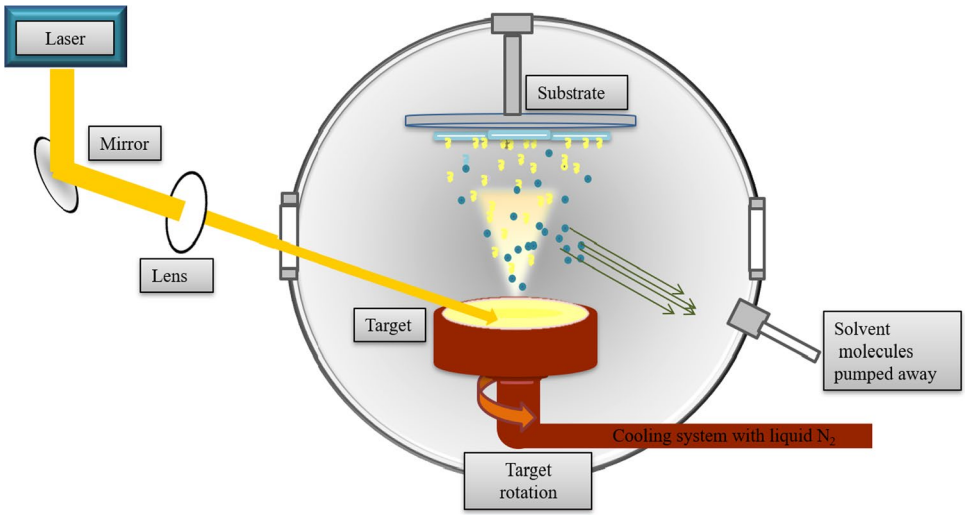

Fig. 2 Scheme of the MAPLE experimental setup

Development Research Institute and approved by the national competent authority.

2.3.2 Animals

All animal experiments are conducted according to the International Standard ISO 10993-10:2010, biological evaluation of medical devices—part 10: tests for irritation and skin sensitization and made under Good Laboratory Practice (GLP) requirement.

Healthy, male New Zealand rabbits (weighing 2.2–2.5 kg, 6 months of age) and healthy adult male Dunkin-Hartley guinea pigs (weighing 300–500 g, 10–16 weeks of age) are provided by Băneasa Animal Facility area for rabbits and guinea pigs of "Cantacuzino" National Medical-Military Development Research Institute, Bucharest. All aspects related to animal housing and care are undertaken in accordance with the national and international regulations concerning animal testing. The breeding system is conventional, and the health monitoring is done according to the Federation of European Laboratory Animal Science Associations (FELASA) recommendations, all animals being negative for the specified pathogens. Throughout the study, the animals are kept under controlled conditions: artificial light 12 of 24 h, temperature of 18 °C ± 2°, relative humidity between 45 and 65% and they received standard pellets food (Cantacuzino Institute, Romania) and water ad libitum. The animals are inspected daily for health status. The rabbits are kept individually in 713 × 716 × 115 mm stainless steel cages (Tecniplast spa, Italia) and the guinea pigs 5 animals per 612 × 435 × 216 mm polycarbonate cages, (Tecniplast spa, Italia). Acclimation period is 7 days prior to the beginning of the experiment.

2.4 Evaluation of patches

2.4.1 Physical–chemical investigations

Given the multiple considerations and complexity in the design of a transdermal therapeutic system, we have been studying both the physical and chemical properties of the polymer blend and drug as thin films together with the compatibility of the laser engineered thin films with the skin.

Atomic force microscopy (AFM) measurements are carried out with an XE 100 AFM setup from Park Systems working in non-contact mode. Commercial silicon cantilevers are used (OMCL-AC240TS, Olympus cantilevers), with 70 kHz nominal resonance frequency and 2 N/m nominal force constant.

The as-deposited polymer blend: drug films morphology, as well as the root mean square roughness (RMS) on several different areas and dimensions, i.e., from 5 μm × 5 μm to 40 μm × 40 μm are determined.

In order to check for any chemical changes on the surface of the laser engineered thin films, the infrared spectra of the native molecules are measured and compared with the thin film spectra. Fourier transform infrared spectroscopy (FTIR) measurements are carried out with a Jasco FT/IR-6300 type A spectrometer in the range 400–4000 cm^{-1}. All spectra are obtained by absorption measurements, accumulating 128 scans, and CO_2/H_2O correction.

The wettability of the deposited thin films is investigated by measuring the contact angles with the sessile drop technique, by depositing a drop of liquid onto the film surface. The drop is imaged and the resulting contact angle is determined by drop shape image analysis calculation. The instrument used is a CAM101 optical system (KSV Instrument Ltd.). The contact angle measurements are carried out in open air, at a room temperature of 22 ± 2 °C by using water. The volume of the water droplets is 1.5 ± 0.2 μl. Three droplets are deposited at different regions of the same film. The contact angle is averaged over three measurements.

2.4.2 Drug release studies

The determination of the drug release rate is a very important study which gives an indication on the sustained release performance of the as-deposited MAPLE films together with the duration of the drug release.

To study the drug release profile of the as-deposited MAPLE polymer blend: drug films, they have been immersed in 100 mL phosphate-buffered saline solution (PBS, pH 7.4) at 37 °C. At pre-determined time intervals, 1 mL of solution is withdrawn and an equal amount of PBS is added (pH 7.4 at 37 °C). The Cp content within the extracted volume is analyzed with a Perkin-Elmer UV–Vis spectrophotometer by the absorbance at 200 nm [33]. All experiments are carried out in triplicate and the mean values are calculated. Further on, the data obtained is fitted with different models, i.e., Higuchi, Hixson–Crowell, Korsemeyer–Peppas, etc. in order to shed light on the mechanisms governing the captopril release kinetics from the MAPLE deposited films.

2.4.3 In vivo tests: skin irritancy

The first test carried out is the evaluation of the skin irritancy of the polymer blend: drug films obtained by MAPLE. The study is carried out according to the International Standard ISO 10993-10 biological evaluation of medical devices—part 10: tests for irritation and skin sensitization and was approved by the Ethics Committee of the Cantacuzino Institute.

To evaluate the skin irritancy, the MAPLE fabricated polymer: drug coatings are deposited onto polyimide substrates (2.5 × 2.5 cm each). The control substance is sodium lauryl

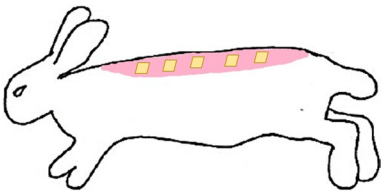

Fig. 3 Representative image of in vivo study displaying patches application process. (i) Shaving the rabbit hair on the back, (ii) patches applied in situ, (iii) patches removed from the back of a rabbit after 24, 48, 72 h

sulphate (SLS). The control substance is diluted to a final concentration of 5%wt in PBS. According to [34] SLS has an irritant potential, and concentrations between 2 and 5% may cause allergic reactions or sensitize the skin.

Three male albino rabbits are used for this study, 6 months old, 2200–2500 g each. 18 h prior to the experiments the fur of the rabbits is shaved to allow the application of the polymer blend: drug films. The MAPLE fabricated polymer blend: drug films are applied in three or five places paravertebrally on each side of every rabbit. Similarly, a control patch is applied either in three or five places of every rabbit paravertebrally. A scheme depicting the application process of the as-deposited MAPLE coatings is shown in Fig. 3.

The rabbits are scored according to the ISO, i.e., if the difference between the average of the MAPLE polymer blend: drug films and the control polymer blend: drug films is smaller or equal to 1, then the MAPLE patches are considered non-irritant.

2.4.4 In vivotests: skin sensitization by Guinea Pig Maximization Test (GPMT)

The second test carried out is the evaluation of the skin sensitization by the Guinea Pig Maximization Test (GPMT) as a result of the application of the as-deposited MAPLE films. The study is conducted according to the International Standard ISO 10993-10: biological evaluation of medical devices—part 10: 2010—tests for irritation and skin sensitization.

The animals used are albino guinea pigs, males (15 animals in total) with weighs between 300 and 500 g. The animals are divided into two groups: a test group and a control group. Prior to each phase of the study, the animals are shaved in the areas where the test substances are applied.

The substances used in this test are: (1) Test sample—polymer film extract from the patches; (2) solvent – methanol; (3) diluent—extra virgin olive oil; and (4) Freund's complete adjuvant (FCA). The study consists of three phases: (1) induction stage 1 (day 0), (2) induction stage 2 (day 7), and (3) the challenge stage (day 21), which shall be described below.

In the intradermal injection phase, the skin of the animals from the control group is injected intradermally (as shown in Fig. 4) with a volume of (A) 0.1 mL of FCA, (B) solvent, (C) 0.1 mL mixture FCA with methanol 50%v/v. Similarly, the skin of the animals from the testing group is injected intradermally (as shown in Fig. 4) with a volume of (A) 0.1 mL of mixture FCA: solvent 50% v/v, (B) sample to test undiluted, (C) 0.1 mL mixture FCA: solvent 50%v/v with the sample to test undiluted 50% v/v.

7 days after the intradermal injection phase, in the induction phase, the test solution is applied on a cotton patch of approx. 8 cm^2 on the shaved skin of the animals in the test group. Similarly, the animal in the control group is treated the same, with solvent. The patches are held firmly in place for 48 h by wrapping the trunk of the animal with elastic bandages.

14 days after the induction phase, the animals are prepared for the challenge phase. A challenge dose is applied topically on the right side (which remained untreated during the induction application) to all the animals in the test group. The left side which had previously received induction applications, is unchallenged. All patches are held in contact with the skin for 24 h before removal.

The skin sites are evaluated using the scoring system for erythema and edema formation of Magnusson and Kligman (ISO 10993-10) [35] for each site challenged. Observations are made 24 and 48 h after initiation of the challenge application and the skin reactions are recorded (Table 1).

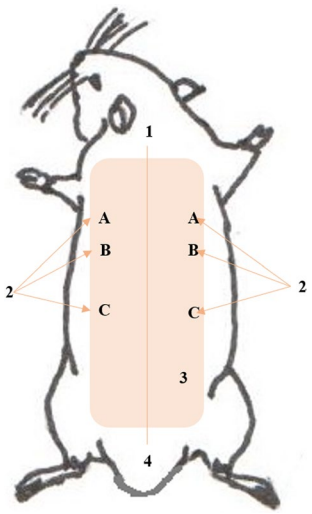

Fig. 4 Injection sites. 1: cranial end; 2: A, B, C, intradermic administration of 0.1 mL; 3: shaved interscapular region; 4: caudal end

Table 1 Classification after Magnusson and Kligman [35]

The reaction after removing patches grading scale	Grading scale
No visible change	0
Discrete or barely perceptible erythema	1
Moderate to severe erythema	2
Severe erythema and/or edema	3

3 Results and discussion

3.1 Morphological investigation of the fabricated patches

The aim of this work is the demonstration of a proof-of-concept transdermal patch fabricated via matrix-assisted pulsed laser evaporation (MAPLE) consisting of a polymer blend: drug for the controlled release of captopril. First, we focus on the morphological investigation of the polymer blend: drug films as-deposited by MAPLE and the potential influence of the surface morphology and topography on the drug release profile.

The first observation is that the hydrophilic/hydrophobic ratio modification within the MAPLE deposited thin films results in morphology and roughness changes. These changes are investigated by a detailed morphological evaluation of the MAPLE deposited thin films via atomic force microscopy (AFM) operating in non-contact mode. The polymer blend: drug AFM images taken on 40 µm × 40 µm areas are shown in Fig. 5 and the root-mean-square (RMS) values (representing the standard deviation of the surface heights) of the scanned surface topography, at the different scan areas are presented in Table 2. The AFM investigations reveal that the as-deposited polymer blend: drug films cover the entire substrate and are free of micrometric cracks. The polymer blend: drug films are dense, and they present micrometric and nanometric formations on the surface as well as small pores (between 70 and 200 nm). Additionally, 10% captopril-containing polymer blend films exhibit a subtly different morphology compared to 1% captopril-containing films, characterized by decreasing roughness values as drug

Table 2 RMS as calculated from the AFM for the HPMC: EC: Cp thin films

MAPLE coatings/ RMS (nm)	No Cp	Cp 1%	Cp 5%	Cp 10%
HPMC80:EC20	248	430	321	240
HPMC60:EC40	330	363	211	166
HPMC40:EC60	227	230	220	160

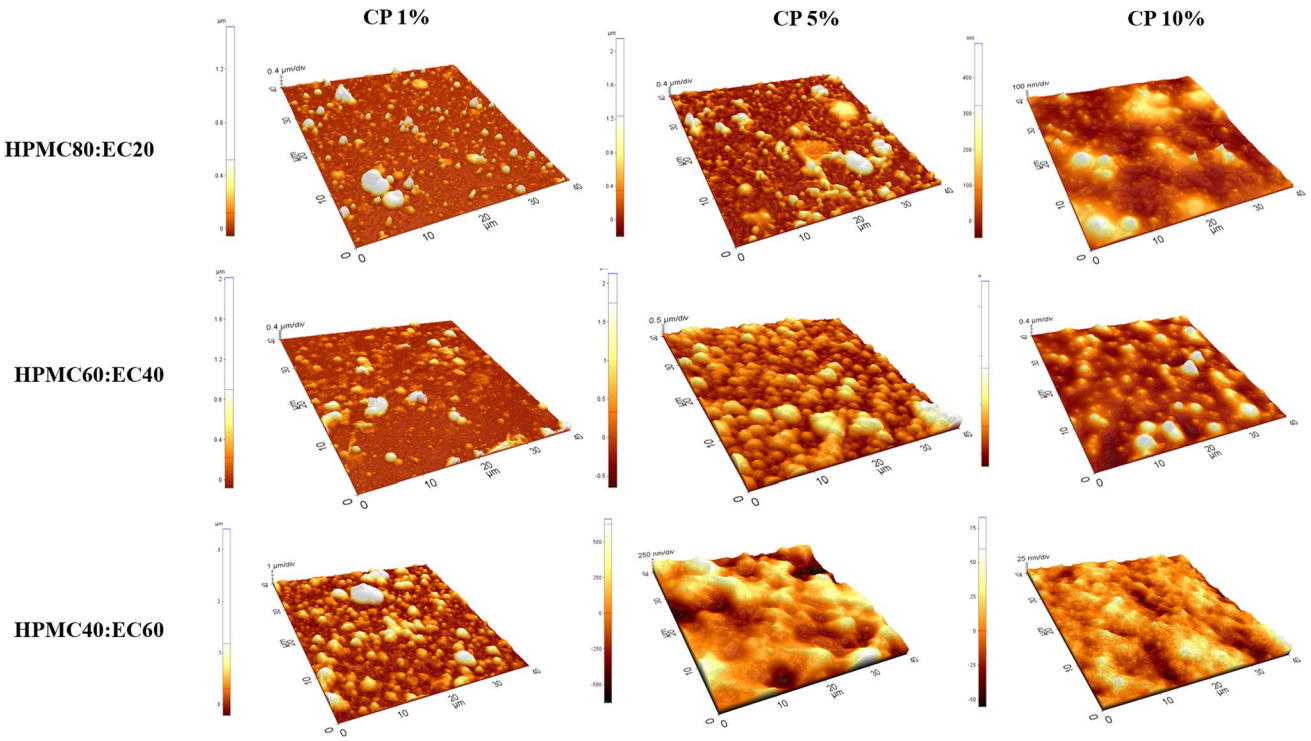

Fig. 5 3D Atomic force microscopy images taken on a 40 µm × 40 µm are of HPMC: EC: Cp thin films deposited by MAPLE

concentration increases, clearly indicating that surface morphology and microstructure can change depending on composition. Furthermore, higher amount of EC leads to films characterized by the presence of nano-domains of spherical form, usually called clusters. In the dynamic simulations, the amount and size of clusters formed during the MAPLE process are influenced by the polymer chain entanglement, which can vary depending on the polymer concentration in the solution. The higher the polymer concentration (or, the higher the entanglement), the larger the clusters form. A coating may become rougher as a result of the deposition of large clusters.

Nano-domains are due to the existence of aggregates or clusters of HPMC chains in the film-forming solution [36] and the hydrophobic interactions between the hydrophobic substituents of HPMC polymer induce the formation of these clusters [37]. For all mixing ratios within the HPMC: EC polymer blends, the films are continuous, with an increased surface structuring and RMS up to 430 nm. The corresponding AFM images also show distinct features for the polymer blend: drug, with the surface RMS roughness results revealing an increased roughness with the increase of HPMC ratio in the HPMC:EC blend incorporating 1% captopril (Table 2). Thus, this is a clear indication that the surface morphology and microstructure changes with the polymer blend: drug composition. The granular structure, characteristic of pure HPMC, preserves when the percentage of captopril increases, leading also to smoother films (as for example HPMC40:EC60: Cp 10%).

In addition to the surface morphology and topography, the surface chemistry of the as-deposited polymer blend: drug films is also important for tailoring the drug release profile. Thus, we apply Fourier transform infrared spectroscopy (FTIR) to study the characteristic vibrations of the functional groups in the MAPLE-deposited films. The FTIR measurements of unprocessed HPMC, EC, and Cp together with the different polymer: drug films deposited by MAPLE are shown in Fig. 6. The HPMC spectra reveals both the broad spectra of the stretching vibration of O–H at 3446 cm^{-1} as well as the stretching of the C–O–C

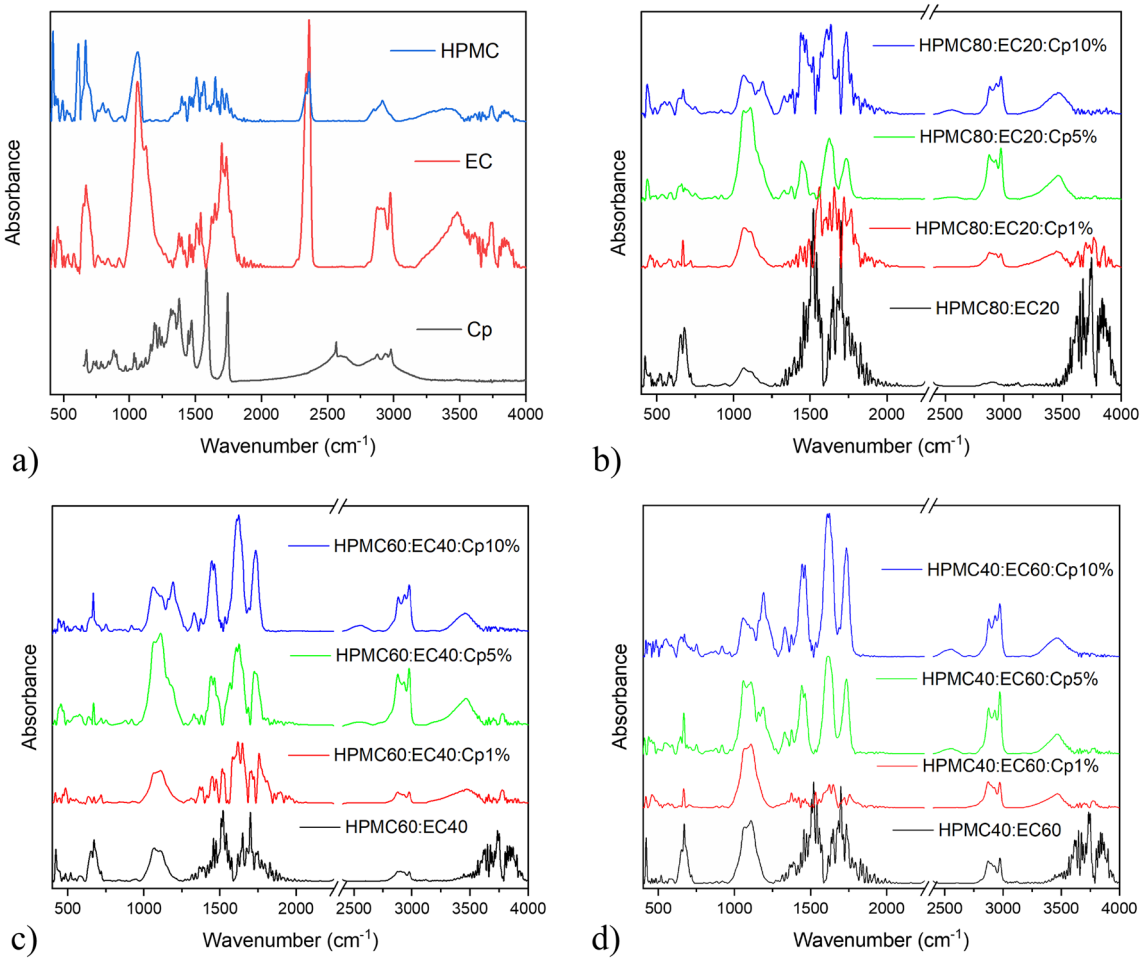

Fig. 6 FTIR spectra of different HPMC: EC: Cp films deposited by MAPLE

anhydroglucose ring at 1054 cm^{-1}, similar to those reported for HPMC [38]. The FTIR spectra of EC (see Fig. 6a) shows the characteristic peaks at 2974 cm^{-1} and 2869 cm^{-1} due to C–H stretching vibration peak. The –OH stretching vibration peak is observed at 3485 cm^{-1}. The peaks at 1091 cm^{-1}, and 1373 cm^{-1} correspond to C–O–C stretching and C–H bending respectively [39]. Furthermore, in the captopril powder spectra shown in Fig. 6a, the peaks at 2981 and 2949 cm^{-1} are assigned to the asymmetric CH_3 and CH_2 stretching vibration, whilst the peak at 2877 cm^{-1} is due to the symmetric CH_3 stretching mode. The peak at 2567 cm^{-1} corresponds to the SH stretching vibration, while the peaks at 1747 and 1591 cm^{-1} are assigned to the C=O stretching vibration of carboxylic acid and amide band, respectively. The peaks at 1469 cm^{-1} and 1385 cm^{-1} is due to the asymmetric and symmetric CH_3 bending vibrations, and the peak at 1333 cm^{-1} is assigned to the OH bending vibration. Finally, the peaks at 1228 cm^{-1} and 1200 cm^{-1} corresponded to the C–O and/or CN stretching vibrations [40–42]. The acquired spectra of the different ratios HPMC: EC films (i.e., 80:20, 60:40, and 40:60 respectively), shown in Fig. 6b–d, are similar to those reported in Ref. [43]. In the FTIR spectra of MAPLE-deposited HPMC:EC, the characteristic bands of HPMC and EC clearly appear.

For all the HPMC:EC films, the same bands may be seen in the spectra, although they are of different intensity, which may be attributable, at least in part, to the differences in the HPMC:EC film thickness.

The spectra recorded in Fig. 6 indicates that there is no significant change in the absorbance peaks of the mixture compared to individual polymers, therefore, it is suggested that no interaction occurred between the two polymers. Moreover, the IR spectra of the MAPLE deposited HPMC: EC: Cp films show that the polymer blend: drug films have not suffered any structural changes during MAPLE, and that there is no significant chemical modification between captopril and the two polymers used.

Furthermore, the wettability as well as the combined action between wettability and surface morphology of the polymer blend: drug films obtained by MAPLE is of major importance for the biocompatibility of a surface. The variation of the HPMC: EC: Cp films static contact angles with the modification of the drug loading is shown in Fig. 7. The contact angle of polymer blends decreases with the increase of the HPMC concentration and the decrease of the EC concentration. This tendency is attributed to the reduction of CH_3 groups from the film surface. Indeed, for pure ethyl cellulose, a contact angle of 84.5° has been observed previously [44] and the more hydrophobic groups there are in the polymeric chains, the films are unable to provide the hydrophilic property. The highest wettability values were obtained for films produced with increased EC amounts, respectively 40 and 60. It is possible to explain this result

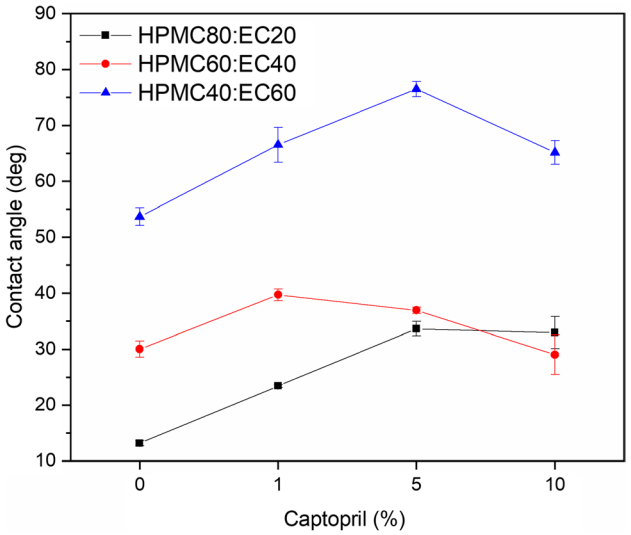

Fig. 7 Static contact angles measured on the HPMC: EC: Cp films deposited by MAPLE as function of concentration of captopril. The lines between points are guides to the eyes

by the greater granularity of the surfaces of these films (see Fig. 5). A decrease in wettability occurs as the granularity of the film surface increases. As the film's amount of contact with water decreases, different adhesion forces are generated, which are not strong enough to overcome the cohesion forces between water molecules. Furthermore, in these films, water access to EC hydroxylic groups is hampered due to the establishment of numerous hydrogen bonds between the cellulose chains. Thus, there is greater exposure of the axial direction of the glucopyranose ring, which is hydrophobic due to the C-H bonds between the pyranoside groups [45, 46]. Taking into account the classification of the contact angle, values between 0° and 90° indicate surfaces susceptible to wetting, all the polymer blends present a rather hydrophilic character. As a result of incorporating captopril into composites, the values of contact angles tended to increase, except for those containing 10% Cp. This variation in contact angle can be related to the surface morphology, specifically roughness, quite similar for the HMPC60:EC40:Cp10 and HMPC80:EC20:Cp10.

An important investigation carried out in this work is the study of the in vitro drug release profile of the as-fabricated MAPLE polymer blend: captopril films (Fig. 8a–c). The first observation we could make is that captopril release over 24 h from the as-fabricated MAPLE films increases with the increase of hydrophilic HPMC in the films. The HPMC80: EC20 and HPMC60: EC40 films as-deposited by MAPLE show a higher captopril release over 24 h (Fig. 8a, b) as compared to HPMC40:EC60, which show a slower release over 24 h (around 60%) (see Fig. 8c). Films with EC60 showed more prominent granularity (Fig. 5). The presence of HPMC between 60 and 80 in the film's composition, prevented

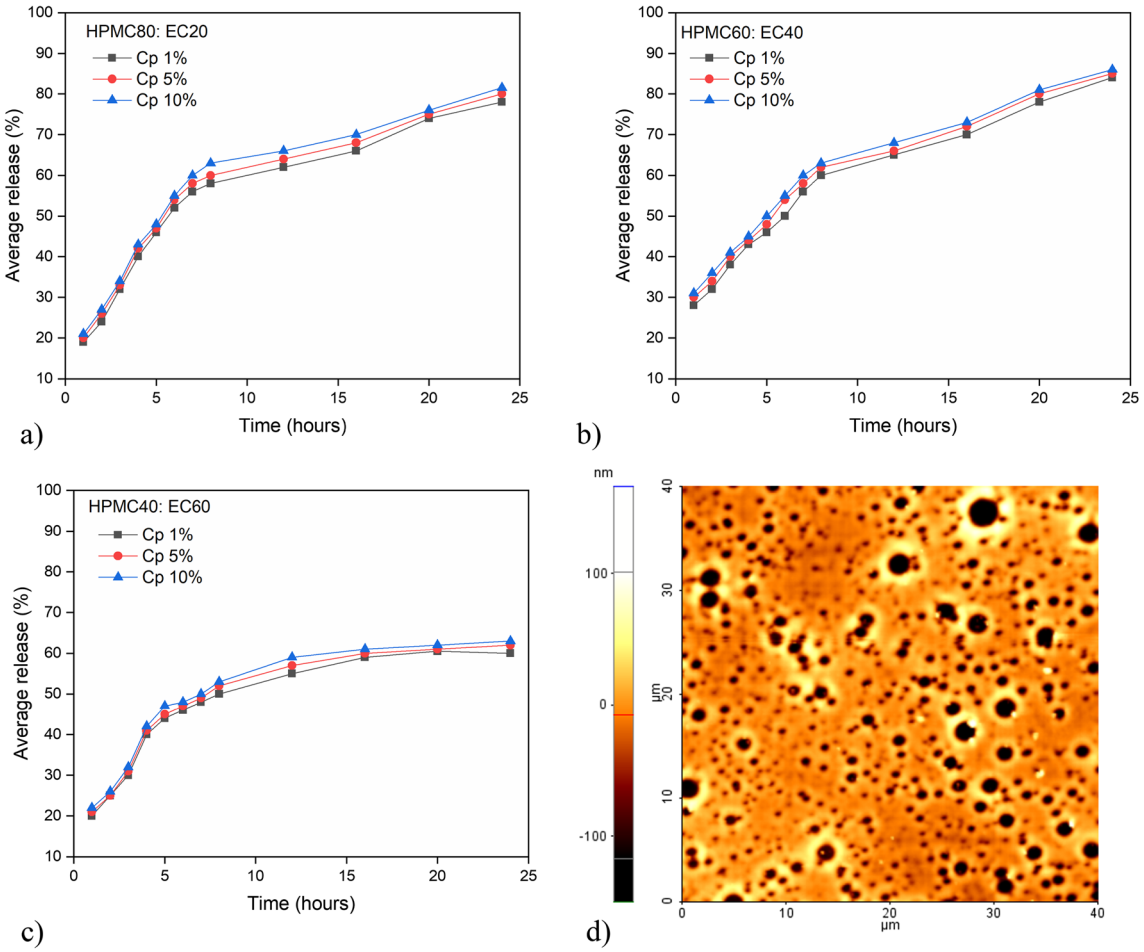

Fig. 8 **a**–**c** Average captopril release from different HPMC: EC films fabricated via MAPLE, **d** AFM image of HPMC60: EC40: Cp1 after 24 h of immersion in PBS

the formation of EC aggregates in larger dimensions and allowed the formation of layers. Furthermore, smaller diameters of the EC also contribute to a decrease in porosity due to the filling of empty spaces in the matrix. Upon contact with water, HPMC undergoes hydration, transitioning from a vitreous to an elastic state, resulting in the formation of a gel [46]. HPMC has a large amount of hydroxyl groups on its surface, which absorbs large amounts of molecules and disperse the matrix [47]. It has been found that EC in the HPMC matrix allows degradation in water to be reduced since cellulose is insoluble in water because of its crystallinity [48]. Furthermore, the hydrogen bonds formed by hydroxylic groups in the EC network and matrix are more robust and stable [49], reducing the degradation in the water of the films. Corroborating this, Larsson et al. [50] stated that structures composed of HPMC and EC suffer dissociation of EC and HPMC network, with the water entry into empty spaces. Thus, the hydrated HPMC will be diluted to lower concentrations and may untangle and diffuse out of the films.

The in vitro captopril release profile of all MAPLE fabricated patches shows an initial burst release, followed by a slow release of the drug. The initial burst release could be attributed to the release of captopril close to the surface of the films [51].

To better understand the mechanism of captopril release from the as-deposited HPMC: EC MAPLE films, the average percentage release of captopril is fitted into different models with the purpose of understanding the mechanism of drug diffusion from the patches. The models applied are compared by calculating the squared correlation coefficient (R^2) value. We found that the data follow the Korsemeyer–Peppas kinetic model [52], which describes the drug release from a polymer system equation.

The Korsmeyer–Peppas Eq. (1) is [52]:

$$M_t/M_\infty = k_{\mathrm{kp}} t^n. \tag{1}$$

In Eq. (1), M_t represents the amount of drug released at time t, M_∞ represents the amount of drug released after ∞

period, k_{kp} is the Korsmeyer–Peppas release rate constant, whilst the value n characterizes the release mechanism of the drug, i.e., $n < 0.45$ the drug transport mechanism is Fickian diffusion, for $n = 1$, case II transport occurs leading to the zero-order release and for $0.45 < n < 1$ non-Fickian diffusion occurs.

The data obtained for captopril release from the HPMC: EC films obtained by MAPLE by applying the Korsmeyer–Peppas model is shown in Table 3.

As it can be observed from Table 3, the HPMC60: EC40: Cp10 together with HPMC40: EC60: Cp5 and HPMC40: EC60: Cp10 indicate the case II transport model. As it has been reported previously [53], this release mechanism occurred through the polymer dissolution controlled and polymeric chain expansion or polymer relaxation/swelling [53].

In contrast, the HPMC 80: EC20 films and HPMC60: EC40 with Cp1 and Cp5 films show a sustained release of captopril over 24 h, i.e., over 80, which is due to the diffusion mechanism, similar to the work reported in Refs. [51, 54]. The validity of this assumption is also based on the AFM image taken on a HPMC60: EC20: Cp1 sample after 24 h of Cp release in the PBS medium, shown in Fig. 8d. After 24 h of drug release in PBS, large pores can be seen on the surface of the HPMC60: EC40:Cp1 sample, which explain the enhanced drug release. The diffusion mechanism is based on the fact that the captopril transport from the HPMC:EC blend into the PBS medium is due to a concentration gradient. In particular, the difference in the concentration gradient leads to captopril release.

Thus, the MAPLE fabricated polymer blend: drug are efficient captopril release systems, which represent an advantage for the treatment of chronic conditions such as hypertension.

Table 3 Captopril release kinetics. The data is obtained by applying the Korsmeyer–Peppas model [52]

Sample	R^2	k_{kp}	n	Release mechanism
HPMC80: EC20: Cp1	0.98	27.82	0.33	Fickian diffusion
HPMC80: EC20: Cp5	0.98	29.29	0.32	Fickian diffusion
HPMC80: EC20: Cp10	0.97	30.42	0.31	Fickian diffusion
HPMC60: EC40: Cp1	0.99	26.40	0.36	Fickian diffusion
HPMC60: EC40: Cp5	0.99	28.34	0.34	Fickian diffusion
HPMC60: EC40: Cp10	0.00	0.85	1.03	Case II transport
HPMC40: EC60: Cp1	0.97	28.78	0.25	Fickian diffusion
HPMC40: EC60: Cp5	0.99	0.96	1.04	Case II transport
HPMC40: EC60: Cp10	0.99	0.85	1.02	Case II transport

3.2 In vivo evaluation of the MAPLE fabricated transdermal patches

3.2.1 Skin irritation studies

The results for skin irritation studies are depicted in Table 4. From the results it has been observed that no erythema and edema were observed on any of the rabbits at the place of application of the test substance and control at 24, 48 and 72 h after inoculation (Fig. 9). In accordance with the International Standard ISO 10993-10, the requirements for testing are met if the final score of the difference between the test substance and the control substance is ≤ 1.0. The end result of this test was − 1.76. Under the test conditions according to this study, the test substance is considered a non-irritating substance.

3.2.2 Guinea Pig Maximization Test (GPMT)

Following the skin sensitization test, none of the animals under study had any abnormal clinical signs during the 25 days of the entire test period. No sensitization was noted among the guinea pigs that were challenged with transdermal patch or the placebo patch. Erythema and edema were not observed after the challenge in this experiment. Thus, according to this study, the MAPLE fabricated patches are considered to have a non-sensitizing effect on the skin.

4 Conclusions

In this study, matrix-assisted pulsed laser evaporation (MAPLE) has been applied for the realization of polymer: drug blends for the controlled release of captopril. The polymer: drug thin films have been obtained by depositing

Table 4 Results of examination of rabbits for test substance and control substance

Rabbit	Test			Control		
	24 h	48 h	72 h	24 h	48 h	72 h
1	0	0	0	4	4	4
2	0	0	0	2	2	2
3	0	0	0	1	2	2
Total	0			23		
Average (total/13)	0			1.76		
Difference	− 1.76					

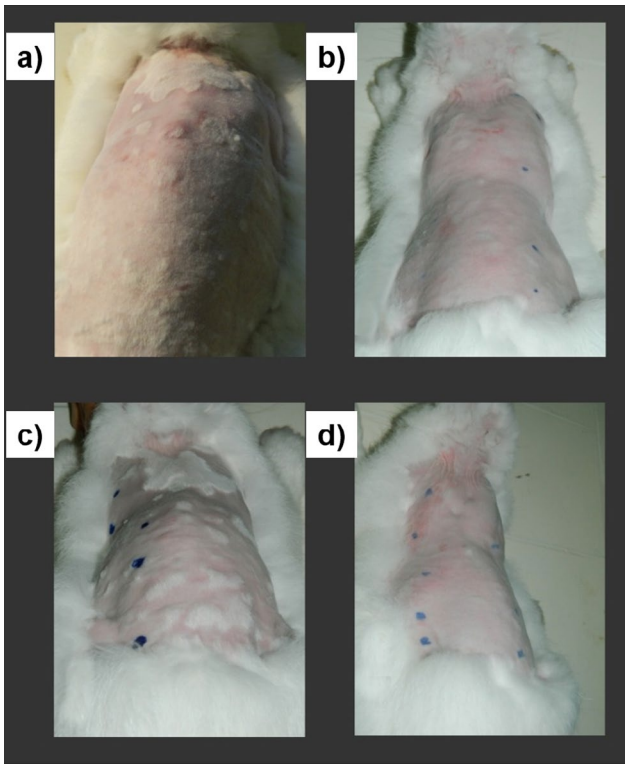

Fig. 9 Rabbit skin **a** before the administration of the as-fabricated MAPLE patch and **b** 24 h, **c** 48 h, and **d** 72 h after the administration of the as-fabricated MAPLE patch

hydroxypropyl methylcellulose (HPMC): (EC) ethyl cellulose blends loaded with different captopril concentrations. The approach followed in this work is quite straight forward, i.e., polymer: drug blends can be directly deposited onto flexible supports by MAPLE without the need for prior surface functionalization or preparation of the surface.

Surface characterization of the resulting films via infrared spectroscopy, atomic force microscopy, and contact angle measurements, corroborated that HPMC: EC: Cp films were deposited without any chemical modifications of their structure. In addition, the HPMC: EC: Cp films as-deposited by MAPLE show a good potential for transdermal drug delivery. The skin irritation studies carried out on rabbits, showed no noticeable skin reactions, thus pointing out the compatibility of captopril with both the polymer blend and with the skin. Last, no skin sensitization was noted among the guinea pigs that were challenged with the MAPLE fabricated transdermal patches.

Therefore, this study has demonstrated that the polymer: drug films fabricated via MAPLE could be significant alternatives for the delivery of captopril. Although this study may be considered a "proof-of-concept" study, we can state that the investigations carried out herein could have applications in other studies, such as the fabrication of therapeutic systems with similar drugs.

Acknowledgements Financial support from the Romanian Ministry of Research, Innovation and Digitalization under Romanian National Core Program LAPLAS VII—contract no. 30N/2023, and UEFISCDI, through projects PN-II-RU-TE-2011-3-0267 and PN-III-P4-ID-PCE-2020-2375 is gratefully acknowledged. The authors would like to thank Dr. Ionut Tirca for acquiring part of the polymer: drug thin films by MAPLE and Dr. Valentina Mărăscu for acquiring the FTIR spectra.

Data availability The data supporting this study's findings are available from the corresponding author upon reasonable request.

Declarations

Conflict of interest The authors declare no competing financial interest.

References

1. M.N. Pastore, Y.N. Kalia, M. Horstmann, M.S. Roberts, Br J Pharmacol. **172**(9), 2179–2209 (2015)
2. D. Bird, N.M. Ravindra, Med Devices Sens. **3**, e10069 (2020)
3. Y.Q. Yu, X. Yang, X.F. Wu, Y.B. Fan, Front. Bioeng. Biotechnol. **9**, 646554 (2021)
4. S. Korani, S. Bahrami, M. Korani, M. Banach, T.P. Johnston, A. Sahebkar, Lipids Health Dis. **18**(1), 193 (2019)
5. I. Singh, A.P. Morris, Int J Pharm Investig. **1**(1), 4–9 (2011)
6. T. Tanner, R. Marks, Skin Res. Technol. **14**, 249–260 (2008)
7. T. Unger, C. Borghi, F. Charchar, N.A. Khan, N.R. Poulter, D. Prabhakaran, A. Ramirez, M. Schlaich, G.S. Stergiou, M. Tomaszewski, R.D. Wainford, B. Williams, A.E. Schutt, Hypertension **75**, 1334–1357 (2020)
8. T.D. Giles, B.J. Materson, J.N. Cohn, J.B. Kostis, J. Clin. Hypertens. **11**, 611–614 (2009)
9. D.R. Gullick, W.J. Pugh, M.J. Ingram, P.A. Cox, G.P. Moss, Drug Dev. Ind. Pharm. **36**(8), 926–932 (2010)
10. D.A. Smith, K. Beaumont, T.S. Maurer, L. Di, J. Med. Chem. **61**(10), 4273–4282 (2018)
11. A. Ahad, M. Aqil, K. Kohli, Y. Sultana, M. Mujeeb, A. Ali, Asian J. Pharm. Sci. **5**, 276–288 (2010)
12. K.A. Walters, K.R. Brain, Dermatological formulation and transdermal systems, in *Dermatological and transdermal formulations*. ed. by K.A. Walters (Informa, New York, 2002), pp.319–400
13. S. Güngör, Y. Ozsoy, Ther. Deliv. **3**(9), 1101–1116 (2012)
14. E. Verhoeven, C. Vervaet, J.P. Remon, Eur. J. Pharm. Biopharm. **63**, 320–330 (2006)
15. R. Enayatifard, M. Saeedi, J. Akbari, Y. HaeriTabatabaee, Trop. J. Pharm Res. **8**(5), 425 (2009)
16. M.J. Vasques, B. Perez-Marcus, J.L. Gomez-Amora, R. Martinez-Pacheo, C. Souto, A. Concheiro, Drug Dev. Ind. Pharm. **18**, 1355–1375 (1992)
17. Y. Okuda, Y. Irisawa, K. Okimoto, T. Osawa, S. Yamashita, Int. J. Pharm. **423**(2), 351–359 (2012)
18. X.-Y. Shi, T.-W. Tan, Biomaterials **23**(23), 4469–4473 (2002)
19. A. Arunachalam, M. Karthikeyan, V.D. Kumar, M. Prathap, S. Sethuraman, S. Ashutoshkumar, S. Manidipa, Curr. Pharma Res. **1**(1), 70–81 (2010)
20. G. Raj, R. Raveendran, *Introduction to Basics of Pharmacology and Toxicology Volume 1: General and Molecular Pharmacology: Principles of Drug Action* (Springer Nature Singapore Pte Ltd., Singapore, 2019)
21. P.K. Wu, J. Fitzgerald, A. Pique, D.B. Chrisey, R.A. McGill, Mater. Res. Soc. Symp. Proc. **617**, J2.3.1-6 (2000)
22. J. Schou, Appl. Surf. Sci. **255**, 5191 (2009)

23. C. Constantinescu, A. Palla-Papavlu, A. Rotaru, P. Florian, F. Chelu, M. Icriverzi, A. Nedelcea, V. Dinca, A. Roseanu, M. Dinescu, Appl. Surf. Sci. **255**, 5491 (2009)
24. A.T. Sellinger, E.M. Leveugle, K. Gogick, L.V. Zhigilei, J.M. Fitz-Gerald, J. Vacuum Sci. Technol. A **24**, 1618 (2006)
25. Y. Wang, H. Jeong, M. Chowdhury, C.B. Arnold, R.D. Priestley, Polym. Cryst. **1**, e10021 (2018)
26. D.B. Chrisey, A. Piqué, R.A. McGill, J.S. Horwitz, B.R. Ringeisen, D.M. Bubb, P.K. Wu, Chem. Rev. **103**(2), 553 (2003)
27. N.L. Dumitrescu, M. Icriverzi, A. Bonciu, P. Florian, A. Moldovan, A. Roseanu, L. Rusen, V. Dinca, F. Grama, Int. J. Mol. Sci. **23**, 3988 (2022)
28. A. Palla-Papavlu, V. Dinca, M. Dinescu, F. Di Pietrantonio, D. Cannatà, M. Benetti, E. Verona, Appl. Phys. A **105**, 651–659 (2011)
29. R. Cristescu, A. Doraiswamy, T. Patz, G. Socol, S. Grigorescu, E. Axente, F. Sima, R.J. Narayan, D. Mihaiescu, A. Moldovan, I. Stamatin, I.N. Mihailescu, B. Chisholm, D.B. Chrisey, Appl. Surf. Sci. **253**, 7702 (2007)
30. I.A. Paun, V. Ion, A. Moldovan, M. Dinescu, Appl. Phys. Lett. **96**, 243702 (2010)
31. A.P. Caricato, V. Arima, M. Catalano, M. Cesaria, P.D. Cozzoli, M. Martino, A. Taurino, R. Rella, R. Scarfiello, T. Tunno, A. Zacheo, Appl. Surf. Sci. **302**, 92–98 (2014)
32. D.A. Cristian, F. Grama, R. Papagheorghe, S. Brajnicov, V. Ion, S. Vizireanu, A. Palla-Papavlu, M. Dinescu, Appl. Phys. A **125**, 424 (2019)
33. H.G. Brittain, H. Kadin, Pharm. Res. **7**, 1082–1085 (1990)
34. C.H. Lee, H.I. Maibach, Contact Dermatitis **33**(1), 1–7 (1995)
35. B. Magnusson, A.M. Kligman, J. Investig. Dermatol. **52**, 268–276 (1969)
36. A. Fahs, M. Brogly, S. Bistac, M. Schmitt, Carbohydr. Polym. **80**(1), 105–114 (2010)
37. N.A. Camino, O.E. Pérez, C. Carrera Sanchez, J.M. Rodriguez Patino, A.M.R. Pilosof, Food Hydrocolloids **23**(8), 2359–2368 (2009)
38. N.K. Anuar, W.T. Wui, D.K. Ghodgaonkar, M.N. Taib, J. Pharm. Biomed. Anal. **43**(2), 549–557 (2007)
39. M.K. Trivedi, A. Branton, D. Trivedi, G. Nayak, R.K. Mishra, S. Jana, J. Biomed. Mater. Res. **3**(6), 83–91 (2015)
40. S. Cavalu, S. CintaPinzaru, V. Chis, Rom. J. Biophys. **17**(3), 195–203 (2007)
41. H. Jancovics, C. Pettinari, F. Marchetti, E. Kamu, L. Nagy, S. Troyanov, L. Pellerito, J. Inorg. Biochem. **97**, 370–376 (2003)
42. A. Palla-Papavlu, L. Rusen, V. Dinca, M. Filipescu, T. Lippert, M. Dinescu, Appl. Surf. Sci. **302**, 87–91 (2014)
43. P.E. Luner, E. Oh, Colloids Surf. A **181**, 31 (2001)
44. L. Li, S. Roethel, V. Breedveld et al., Cellulose **20**, 3219–3226 (2013)
45. P.C. Faria-Tischer, C.A. Tischer, L. Heux et al., Mater. Sci. Eng. C Mater. Biol. Appl. **51**, 167–173 (2015)
46. T. Kiss, T. Alapi, G. Varga, C. Bartos, R. Ambrus, P. Szabo-Revesz, G. Katona, J. Pharm. Sci. **108**(8), 2552–2560 (2019)
47. M. Ci, J. Liu, S. Shang, Z. Jiang, P. Zhu, S. Sui, Fibers Polym. **21**, 2179–2185 (2020)
48. S. Belbekhouche, J. Bras, G. Siqueira, C. Chappey, L. Lebrun, B. Khelifi, S. Marais, A. Dufresne, Carbohydr. Polym. **83**, 1740–1748 (2011)
49. S. Van Nguyen, B.K. Lee, Cellulose **28**, 5693–5705 (2021)
50. M. Larsson, A. Johnsson, S. Gårdebjer, R. Bordes, A. Larsson, Mater. Des. **122**, 414–421 (2017)
51. H. Bera, Y.F. Abbasi, V. Gajbhiye, K.F. Liew, P. Kumar, P. Tambe, A.K. Azad, D. Cun, M. Yang, Mater. Sci. Eng. C **110**, 110628 (2020)
52. R.W. Korsmeyer, R. Gurny, E. Doelker, P. Buri, N.A. Peppas, Int. J. Pharm. **15**(1), 25–35 (1983)
53. A.K. Azad, S.M.A. Al-Mahmood, B. Chatterjee, W.M.A. Wan Sulaiman, T.M. Elsayed, A.A. Doolaanea, Pharmaceutics **12**, 219 (2020)
54. M.S. Latif, A.K. Azad, A. Nawaz, S.A. Rashid, M.H. Rahman, S.Y. Al Omar, S.G. Bungau, L. Aleya, M.M. Abdel-Daim, Polymers **13**, 3455 (2021)